Biomaterials Science

Dual-stage growth factor release within 3D protein-engineered hydrogel niches promotes adipogenesis

Journal:	*Biomaterials Science*
Manuscript ID:	BM-ART-04-2014-000142.R1
Article Type:	Paper
Date Submitted by the Author:	13-Jun-2014
Complete List of Authors:	Greenwood-Goodwin, Midori; Stanford University, Bioengineering Teasley, Eric; Stanford University, Bioengineering Heilshorn, Sarah; Stanford University, Materials Science & Engineering; Stanford University, Bioengineering

SCHOLARONE™
Manuscripts

Biomaterials Science

ARTICLE

Dual-stage growth factor release within 3D protein-engineered hydrogel niches promotes adipogenesis

Midori Greenwood-Goodwin,[a] Eric S. Teasley,[a] and Sarah C. Heilshorn[a,b]

Engineered biomimetic microenvironments from hydrogels are an emerging strategy to achieve lineage-specific differentiation *in vitro*. In addition to recapitulating critical matrix cues found in the native three-dimensional (3D) niche, the hydrogel can also be designed to deliver soluble factors that are present within the native inductive microenvironment. We demonstrate a versatile materials approach for the dual-stage delivery of multiple soluble factors within a 3D hydrogel to induce adipogenesis. We use a Mixing-Induced Two-Component Hydrogel (MITCH) embedded with alginate microgels to deliver two pro-adipogenic soluble factors, fibroblast growth factor 1 (FGF-1) and bone morphogenetic protein 4 (BMP-4) with two distinct delivery profiles. We show that dual-stage delivery of FGF-1 and BMP-4 to human adipose-derived stromal cells (hADSCs) significantly increases lipid accumulation compared with the simultaneous delivery of both growth factors together. Furthermore, dual-stage growth factor delivery within a 3D hydrogel resulted in substantially more lipid accumulation compared to identical delivery profiles in 2D cultures. Gene expression analysis shows upregulation of key adipogenic markers indicative of brown-like adipocytes. These data suggest that dual-stage release of FGF-1 and BMP-4 within 3D microenvironments can promote the *in vitro* development of mature adipocytes.

Introduction

Stem cells are a promising cell source for potential regenerative medicine applications; however, robust induction of stem cell differentiation toward a defined cell type remains challenging. Stem cell differentiation *in vivo* occurs in specialized stem cell niches, which are inductive microenvironments with tightly regulated signaling mediated by soluble molecules, cell-cell interactions, and cell-extracellular matrix (ECM) interactions.[1,2] In contrast, induction of stem cell differentiation *in vitro* is typically achieved by presenting soluble factors or by direct transcriptional regulation. The development of biomimetic microenvironments with robust control over cell differentiation will be useful for tissue engineering applications, *in vitro* models of disease progression and drug discovery.[3-6] Engineered biomimetic microenvironments from hydrogels are an emerging strategy for addressing the challenges in lineage-specific differentiation *in vitro*.[8,9] These microenvironments typically utilize hydrogels to provide biochemical and biophysical cues that mimic the native inductive microenvironment.[10] One strategy to fine-tune the presentation of these cues is the design of multifunctional protein-engineered hydrogels.[11] Here we describe the development of a protein-engineered hydrogel system with temporally controlled release of two soluble factors to induce robust *in vitro* adipogenic differentiation.

Mature adipocytes are essential for metabolic homeostasis in all tissues, and *in vitro* studies toward recapitulating the inductive microenvironment for adipogenesis would be useful for modeling adipose tissue development, metabolic homeostasis and associated pathologies, including type II diabetes.[12] Human adipose-derived stromal cells (hADSCs) are an abundant, multipotent cell source isolated from lipoaspirate that can be induced to differentiate into adipocytes.[13,14] Adipogenesis occurs in two functional steps, stem cell commitment followed by terminal differentiation.[15] Despite several studies demonstrating the adipogenic potential of hADSCs, little is known about the synergistic effects of biochemical and biophysical cues regulating the process, especially within 3D biomimetic microenvironments.

Monolayer cultures of hADSCs on both hydrogels and tissue culture plastic display altered phenotypes and genotypes compared to micromass cultures or cells cultured within 3D hydrogels.[16-18] When evaluating previous results from a biochemical perspective, the incorporation of ligands derived from the native ECM enhanced adipogenesis by supporting specific cell-integrin attachment to the engineered hydrogel microenvironment.[19,20] From a biophysical perspective, microenvironments capable of being remodeled by cells, either through the use of physically crosslinked hydrogels or protease-enabled degradation, enhanced adipogenesis by maintaining a rounded cell morphology.[21,22] Therefore, we selected a protein-engineered hydrogel containing the biochemical RGD ligand derived from fibronectin for cell-integrin attachment and that physically crosslinks to enable cell remodeling. Specifically, we utilized a previously designed mixing-induced two-component hydrogel (MITCH).[23] The two components of

MITCH heteroassemble under physiological conditions through specific molecular recognition and hydrogen bonding of complementary peptide domains to form a hydrogel. MITCH is injectable, allows for *in situ* encapsulation of hADSCs, supports hADSC culture *in vitro*, and increases hADSC retention *in vivo*.[23-25]

To customize MITCH for enhanced adipogenic differentiation, we sought to design a system for temporal control over the presentation of soluble factors within the hydrogel. One strategy to deliver soluble factors in 3D microenvironments is the use of microspheres for sustained release.[26,27] Microspheres can be fabricated from various materials,[28-30] using multiple techniques,[32,32] which impact the downstream loading efficiency, release profiles, and bioactivity of the encapsulated soluble factors.[33,34]

Sequential release of multiple growth factors mimicking in vivo temporal profiles in the native inductive microenvironment is expected to enhance stem cell differentiation.[35] The use of sequential release has been explored extensively for tissue vascularization,[36,37] but it is less explored in the design of 3D stem cell inductive microenvironments for adipogenesis. Pro-adipogenic soluble factors, fibroblast growth factor 1 (FGF-1) and bone morphogenetic protein 4 (BMP-4), are good candidate factors for recapitulation of the *in vivo* adipogenic microenvironment. FGF-1 signalling has been shown to promote the first stage of adipogenesis, stem cell commitment toward adipocytes.[38,39] BMP-4 signalling is required for terminal adipocyte differentiation of preadipocytes.[40,41] Importantly, cell treatment with BMP-4 prior to FGF-1 reduces adipogenesis,[42] suggesting that temporally controlled presentation of these factors is important for adipogenic differentiation.

We developed a biomimetic microenvironment using MITCH for co-encapsulation of hADSCs with alginate microgels for temporally controlled release of FGF-1 and BMP-4 for *in vitro* adipogenic differentiation. We hypothesized that release and delivery of FGF-1 from MITCH at early cell culture times in combination with sustained delivery of BMP-4 from microgels would increase the extent of hADSC differentiation toward adipocytes. We show that both the hydrogel properties and temporally controlled release of these two factors increases adipogenic differentiation on a per cell basis.

Experimental section

Microgel formation

Microgels were formed using a glass microfluidic device with channels arranged in a flow-focusing geometry, similar to previous reports.[43-45] To model encapsulation efficiency and release kinetics, the alginate-drug aqueous phase contained 80 mg/ml low viscosity, alginic acid sodium salt from brown algae (Sigma-Aldrich) and 2 mg/ml Dextran-FITC or Dextran Texas Red, dissolved in UltraPure deionized water. To encapsulate and release growth factors, the alginate-drug aqueous phase contained 80 mg/ml low viscosity, alginic acid sodium salt and 0.14 - 2.0 µg/ml human fibroblast growth factor 1 (FGF-1) or human bone morphogenetic protein 4 (BPM-4), dissolved in UltraPure deionized water. The alginate-drug aqueous phase is then sterile filtered prior to use. The oil-surfactant phase contains Span 80 surfactant diluted into Isopar M solvent

(Exxon Mobil Chemical) to a final concentration of 0.25 w/w%. A single channel alginate-drug aqueous phase meets two oil-surfactant phase inputs at a cross junction (Fig. 1a). Micron-sized droplets of the aqueous phase were crosslinked in a 150 – 500 µl divalent ion bath. Crosslinked microgels were collected by 5 minute centrifugation at 1000 rpm and rinsed three times with 150 mM Phosphate Buffered Saline (PBS), pH 7.4.

Microgel characterization

Samples of the alginate microgels (5 µl) were removed and placed in excess PBS on a glass coverslip and imaged using a Photometrics QuantEM camera or CCD camera with an inverted fluorescence microscope (Nikon Elements or Zeiss, respectively). Images of each sample were taken in a grid pattern and analyzed using ImageJ (NIH freeware).[46] Images were stitched together using a plug-in. Individual microgel cross-sectional area and diameter were manually analyzed by digital tracing (Wacom Intuos4 Pen Tablet). Frequency tables of microgel diameters were generated using 10 µm intervals, and histograms were generated from the percentage of microgels in each interval. The distribution of microgel diameters is reported as a mean and standard deviation. The polydispersity of microgel diameters is reported as the coefficient of variance (CV) using the following formula: $CV = (d/S.D.) \times 100\%$, where d is the mean diameter and *S.D.* is the standard deviation of the mean diameter.

Macromolecule loading and release

The macromolecules used include recombinant human fibroblast growth factor 1 (FGF-1, Miltenyi Biotech), recombinant human bone morphogenetic protein 4 (BMP-4, Pepro Tech), Dextran-fluorescein isothiocyanate (FITC, MW of 10, 20, 40 kD, Sigma-Aldrich), and Dextran-Texas Red (MW of 10, 40 kD, Life Technologies).

The unencapsulated concentration of Dextran molecules in the aqueous phase was measured by fluorescence (Multimode Microplate Reader, Model M2, Molecular Dynamics). Similarly, the encapsulated macromolecule concentration was determined by measuring the fluorescence of solutions of microgels degraded in 1.5 M PBS, pH 7.4. The concentration of FGF-1 and BMP-4 was detected using an indirect fluorophore linked immunosorbent assay (FLISA). 50 µl of supernatant was added to individual wells of a high-binding 96 well plate (EIA/RIA plate, Corning). 100 µl of 1:30 antibody dilutions, FGF-1 C-19 primary antibody or BMP-4 antibody N-16, was added to the corresponding sample (Santa Cruz Biotech). Lastly, 1:200 dilutions of secondary antibody, Alexa Fluor® 488 Donkey Anti-Goat IgG (H+L, Life Technologies), was added to each well. Standard curves ranging from 0.002 to 2 µg/ml for each growth factor were used to determine the concentration of unencapsulated, encapsulated, and released growth factors. All samples were measured by fluorescence of the secondary antibody (Multimode Microplate Reader, Model M2, Molecular Dynamics).

Encapsulation efficiency was calculated using the following formula: *Encapsulation efficiency = $(C_t / C_i) \times 100\%$*, where C_t is the total concentration of macromolecule in the alginate suspension post-microgel degradation and C_i is the total concentration of macromolecule in the alginate solution before microgels were formed.

Release profiles were obtained by incubating alginate microgels at 0.05 v/v% in growth media: Dulbecco's Modified Eagle's Medium (DMEM) supplemented with 2 mM L-glutamine, 10 v/v% FBS and 1 v/v% penicillin/streptomycin (Life Technologies). Samples were stored in 1.5 ml Eppendorf tubes at 37 °C in triplicate. 100 µl of sample was collected at each time point and replaced with fresh media.

Bioactivity of growth factors delivered from microgels

FGF-1 and BMP-4 bioactivity was determined by an *in vitro* adipogenesis assay. Human adipose-derived stromal cells (hADSCs) were exposed to alginate microgels with and without growth factors. At day 7, following exposure to alginate microgels, cells were fixed overnight in 4% paraformaldehyde and stained with Oil Red O (Cayman Chemical) for 20 min at room temperature. The positive control was adipogenic induction media: growth media supplemented with dexamethasone, human recombinant insulin, and 3-isobutyl-1-methylxanthine (IBMX) per manufacturer's directions (Cayman Chemical).

Expression and purification of protein-engineered hydrogel (MITCH) components

The engineered proteins were produced using recombinant protein expression and affinity chromatography purification, as previously reported.[23] The DNA sequence encoding the C7 polypeptide was cloned into a pET-15b vector (Novagen), and the polypeptide P9 was cloned into a pJexpress414 vector (DNA2.0). Individual plasmid constructs were transformed into the BL21(DE3) pLysS Escherichia coli host strain (Invitrogen). Recombinant proteins were expressed following isopropyl β-d-1-thiogalactopyranoside (IPTG) induction, purified using specific binding of N-terminal polyhistidine tags to Ni-nitrilotriacetate resin (Qiagen), and buffer exchanged. Recombinant proteins were concentrated by centrifugation across 30 kDa MWCO Amicon Ultracel-10K filter units (Millipore). Protein identity and purity were confirmed by gel electrophoresis and Western blotting.

Microgel encapsulation within MITCH

Microgels (10 µl) were first added to a P9 solution (10 µl, 40 wt% in 150 mM PBS) followed by mixing with a C7 solution (20 µl, 20 wt% in 150 mM PBS) at 37°C, pH 7.4. The resulting bulk hydrogels contain 10 wt% C7, 10 wt% P9 and 10 to 25 v/v% microgels.

Rheology of MITCH

The viscoelastic properties of MITCH with increasing volumes of microgels were determined by dynamic oscillatory rheology experiments and linear shear rheology using a parallel-plate geometry, diameter = 8 mm, gap = 0.15 mm (Anton Paar Physica MCR 301 rheometer). A humidity chamber was placed around the samples to prevent dehydration, and the temperature was maintained at 37 ± 0.02 °C by a Peltier temperature control unit. Hydrogels were directly prepared on the platform. Frequency sweep experiments were performed pre and post shear-thinning experiments. During frequency sweep experiments, the storage (G′) and loss (G″) moduli were monitored from $0.1 - 100$ s^{-1} at a constant strain of 5.7%. During shear-thinning experiments a constant shear rate of 0.1 s^{-1} was applied for 160 s and then increased to 10 s^{-1} for 60 s

(which is sufficient to disrupt the hydrogel network). This was repeated twice and followed by application of a constant shear rate of 0.1 s^{-1} for 180 s before running the post shear-thinning frequency sweep.

In vitro adipogenesis

Cell isolation and culture. Human adipose derived stromal cells (hADSCs) were harvested from human lipoaspirate from the flank and thigh regions and processed as detailed previously.[25] Fresh hADSCs were gifted from Dr. Michael Longaker (Stanford University, CA, U.S.A.). hADSCs were maintained in growth media and used between passages $3 - 5$. Cell passages were maintained at lower than 80% confluency in culture prior to use and reseeded on 100-mm culture dishes (10 ml media; Falcon) at a density of 1×10^6 cells/ml prior to differentiation.

Cell differentiation. For 2D cultures, cells were reseeded into 12-well plates at a concentration of 250,000 cells per well in growth or induction media. For 3D cultures, cells were encapsulated within MITCH to a final concentration of 250,000 cells per gel (final gel volume of 40 µl, d = 6 mm, h = 2.5 mm). Each individual gel was separated into a single well of a 12-well plate and submerged in growth or induction media. For both 2D and 3D cultures, media was exchanged once at day 3 by removing 70% of the bulk media and replacing with fresh growth or induction media without growth factors. Adipogenic differentiation of hADSCs at day 7 was assessed by the presence of intracellular lipid accumulation and by quantitative, reverse-transcription, polymer chain reaction (qRT-PCR).

Lipid accumulation per cell. Lipid accumulation was assessed via Oil Red O staining as described above. The extent of Oil Red O staining was quantified by isopropanol extraction for 30 minutes at room temperature ($22 - 25$°C) followed by absorbance reading at 510 nm (Multimode Microplate Reader, Model M2, Molecular Dynamics). To estimate lipid accumulation per cell, the total Oil Red O absorbance was divided by the total cellular dsDNA, determined by using the Quant-IT PicoGreen dsDNA Kit (Invitrogen). Growth and induction media were removed and replaced with cell lysis buffer: 25 mM Tris-HCl pH 7.4, 2% SDS, 1 mM EDTA, and 5% glycerol. Cell lysate was incubated with dsDNA reagent in TE buffer, pH 8.0, in 2 ml Eppendorf tubes for 2–5 min at RT. 200 µl of the mixture was transferred to a 96-well microplate and the fluorescent intensity was measured on a fluorescence spectrometer (Multimode Microplate Reader, model M2, Molecular Dynamics). Lambda DNA concentrations from 1 ng/ml to 1 µg/ml were used to generate the standard curve (Invitrogen). The fluorescence value of the blank, reagent in TE buffer, was subtracted to generate the standard curve and to calculate the DNA content of all samples.

Quantitative, reverse-transcription, polymerase chain reaction (qRT-PCR). RNA isolation was achieved using TRIzol® Reagent (Ambion) with a Phase Lock Gel (5 PRIME) according to the manufacturer's protocol and quantified by a spectrophotometer (Nanodrop ND-2000c). Synthesis of cDNA was carried out using a High Capacity cDNA Reverse Transcription kit according to the manufacturer's protocol (T100 Thermal Cycler, BIO-RAD). Using serial dilutions of cDNA, qPCR was performed for the genes encoding Leptin, uncoupling protein 1 (UCP1), Glyceraldehyde 3-phosphate dehydrogenase (GAPDH), fatty acid binding protein 4

(FABP4), glucose transporter (GLUT4), CCAAT/enhancer binding protein subunits alpha and beta, (C/EBPα, C/EBPβ), and peroxisome proliferator-activated receptor gamma (PPARγ). Custom primer sequences were previously reported or designed in house for mature mRNA transcripts (IDT, Table S1). Amplification reactions were performed in a total volume of 15 µl PCR mixture containing 7.5 µl Fast SYBR Green Master Mix™ (Applied Biosystems), 0.45 µM of each PCR primer, 1.6 µl dH$_2$O and 5 µl cDNA samples. After initial denaturation at 95 °C for 10 s, targets were amplified using 40 cycles of 95 °C, 10 s, and then 60 °C, 30 s (StepOnePlusTM Real-Time PCR Machine, Applied Bioystems). All samples were analysed in triplicate. Relative mRNA abundance was determined by the 2$^{-\Delta\Delta Ct}$ method, with GAPDH used as the endogenous control.[47]

Statistical analysis

Statistical analyses were carried out using MatLab, Version 8.3 or GraphPad Prism® software Inc., Version 6. Alginate microgel size distributions were assessed using the Kolmogorov-Smirnov test. Encapsulation efficiency, cumulative release curves, and rheology, were assessed for statistical significance using an unpaired t-test. Oil Red O absorbance, total DNA, Oil Red O per total DNA, and qRT-PCR were assessed for statistical significance using one-way ANOVA with Tukey Post-hoc analysis. $p < 0.05$ was considered to be significant for all statistical analyses.

Results and discussion

Alginate microgel formation and encapsulation within MITCH

We developed a hydrogel composite of alginate microgels encapsulated within a Mixing-Induced Two-Component Hydrogel (MITCH) for temporally controlled release of multiple soluble factors (Fig.1a). Uniform aqueous alginate droplets within an oil-surfactant phase were formed in a microfluidic chip that utilizes flow-focusing geometry. These alginate droplets were then crosslinked off-chip in a divalent ion bath. Soluble factors were passively loaded into the alginate microgels by adding the soluble factors to the alginate solution prior to microgel formation.

Alginate microgels were then embedded within a hydrogel by mixing with the two recombinant protein components of MITCH. As reported previously, the two recombinant protein components, C7 and P9, contain 7 and 9 repeats of complementary binding domains, a CC43 WW domain and a proline-rich peptide domain, respectively (Table S2).[23] Physical cross-linking between these complementary binding domains occurs at physiological conditions through specific molecular recognition and hydrogen bonding, forming a hydrogel network within seconds. Soluble factors can also be directly loaded into MITCH by mixing with C7 and P9 during gelation, without prior encapsulation in alginate microgels. Delivery of soluble factors from MITCH results in burst release (Fig. 1b). In contrast, the release rate of soluble factors from MITCH when pre-encapsulated in alginate microgels is significantly reduced, resulting in sustained delivery (Fig.1b). These results demonstrate two distinct temporal release profiles for the delivery of soluble factors from MITCH.

Alginate microgel characterization and soluble factor encapsulation efficiency

To assess the generality of this strategy for encapsulation of a variety of molecules within alginate microgels, we characterized the encapsulation efficiency and alginate microgel size for model macromolecules. Specifically, water-soluble Dextran of two molecular weights with two fluorescent dyes were evaluated. Alginate microgels were crosslinked using divalent ions with variable binding affinities. Crosslinked alginate microgels encapsulated larger, neutral soluble factors with greater efficiency, independent of the divalent ion crosslinking solution (Fig. 2a). The final concentrations of Dextran-fluorescein isothiocyanate (FITC) encapsulation efficiency is significantly greater than Dextran-Texas Red encapsulation efficiency, for both molecular weights tested. The observed difference in encapsulation efficiency most likely results from partitioning of Dextran-Texas Red into the oil phase due to the zwitterionic charge on the Texas Red dye. Additionally, Dextran-FITC and Dextran-Texas Red encapsulation efficiency is significantly decreased with decreasing molecular weight (Fig. 2a). The reduced encapsulation efficiency for lower molecular weight Dextran is unsurprising, presumably due to faster diffusion out of the alginate droplet prior to off-chip crosslinking. Unlike previous reports,[35,48] Dextran encapsulation efficiency in our system is not significantly affected by the type of crosslinking ion (Fig. 2a), suggesting that the concentration of ions, 400 mM, is sufficient to saturate the alginate. Alginate microgels crosslinked with BaCl$_2$ are expected to undergo minimal swelling and have previously demonstrated higher stability in aqueous environments.[48] Therefore, for all future experiments we selected alginate microgels crosslinked in BaCl$_2$ for sustained release of soluble factors.

Alginate microgel size distribution is unaffected by the encapsulation of various soluble factors (Fig. 2b). The coefficients of variance for the microgel diameters ranged from 20.8 – 30.3% (Fig. 2b). Alginate microgels exhibit spherical morphologies in aqueous solution (Fig. 2c). The average alginate microgel diameter across all samples, 66 (± 14) – 74 (± 20) µm, suggests that microgels will be too large for significant cell internalization.[49]

Mechanical properties of MITCH with encapsulated alginate microgels

The mechanical properties of MITCH containing alginate microgels were explored to verify the formation of a soft, bulk hydrogel network for supporting adipocyte differentiation. MITCH gelation is not disrupted by the addition of up to 25 v/v% of alginate microgels to the C7 and P9 components. The mechanical properties of the composite hydrogel are altered with the encapsulation of up to 25 v/v% alginate microgels within MITCH. Bulk oscillatory rheology was used to characterize the impact of alginate microgels on the viscoelastic properties of MITCH. Increasing the volume percent (v/v %) of alginate microgels embedded within MITCH from 0 to 10 to 25 increases the shear modulus of the composite hydrogel (38, 50, and 81 Pa, respectively, Fig. 3a). These results suggest that the more rigid alginate microgels restrict the deformation of MITCH by introducing a mechanical restraint within the composite hydrogel.[50]

Shear rheology was used to determine the shear-thinning and self-healing properties of MITCH with encapsulated alginate microgels. MITCH embedded with 25 v/v% alginate microgels underwent near instantaneous shear-thinning following

application of 10 s^{-1} shear rates, as evidenced by a drop in viscosity greater than two orders of magnitude. When the shear-rate was reduced to 0.1 s^{-1}, the initial viscosity is fully recovered. Shear-thinning of the composite hydrogel is reversible through multiple cycles (Fig. 3b). Additionally, the storage and shear moduli before and after shear-thinning were indistinguishable (Fig. 3c). The reported shear modulus of MITCH embedded with 25 v/v% alginate microgels is similar in magnitude to that reported for adipose tissue (50 to 300 Pa at low strains).[51]

Release kinetics and bioactivity of soluble factors delivered from alginate microgels

To quantify the release kinetics of soluble factors from alginate microgels we examined the release of Dextran-FITC molecules with molecular weights varying from 10 to 40 kD up to three months (Fig. 4a). For all experiments, alginate microgels were suspended in hADSC growth media. As expected, at longer times (up to 3 months), the cumulative release was dependent on the molecular weight, with smaller molecules delivered more rapidly (Fig. 4a). These results suggest that there is minimal erosion and degradation of the alginate microgels over long time periods when cultured in growth media. At short times (up to 7 days), the cumulative release was linear with no dramatic burst release for all molecular weight Dextrans (Fig. 4a, b). This sustained release has previously been attributed to the low swelling of alginate microgels, which prevents rapid diffusion out of the microgels. One advantage of a linear release profile for delivery of growth factors within an *in vitro* microenvironment is that it enables straightforward prediction of the released growth factor concentration at regular time intervals. We further quantified the release kinetics of FGF-1 and BMP-4 from alginate microgels (Fig. 4b). Similar to the Dextran release profiles, cumulative release of both encapsulated growth factors was linear with no observed burst release over 7 days (Fig. 4b). Moreover, we show that encapsulation efficiency is high, 86%, for both FGF-1 and BMP-4 (Fig. 4c).

The bioactivity of growth factors released from alginate microgels was confirmed by *in vitro* induction of adipogenesis (Fig. 5). Alginate microgels containing FGF-1 or BMP-4 were added to induction media and delivered to hADSCs on tissue culture polystyrene (TCPS). We calculated the amount of growth factor loading required to obtain concentrations similar to those used in 2D monolayer cultures, where soluble factors are typically replenished every 2 to 3 days. Pro-adipogenic induction by FGF-1 occurs at concentrations ranging from 1 to 90 ng/ml, with increasing concentrations showing enhanced adipogenesis.[38,52] Therefore, to achieve an estimated concentration of 90 ng/ml at two days, 1.3 μg FGF-1 was loaded into 1 ml of alginate solution. Pro-adipogenic induction by BMP-4 occurs at concentrations ranging from 10 to 50 ng/ml, with little to no concentration dependence.[53] However, in the presence of FGF-1, high effective concentrations of BMP-4 may reduce adipogenesis.[42] Therefore, to achieve an estimated concentration of 10 ng/ml at two days, 0.14 μg BMP-4 was loaded into 1 ml of alginate solution.

For direct comparison of bioactivity between released growth factors and supplemented soluble factors, 90 ng/ml of FGF-1 or 10 ng/ml of BMP-4 were added directly to the induction media at days 0, 3, and 5. Lipid accumulation was measured by Oil Red O staining, and total number of cells was quantified by

total dsDNA content at day 7. Sustained delivery of FGF-1 from alginate microgels showed similar levels of lipid accumulation per cell compared to dose delivery of FGF-1 directly to the media (Fig. 5a). Interestingly, sustained delivery of BMP-4 from alginate microgels resulted in significant enhancement in lipid accumulation per cell (p < 0.01), suggesting that sustained release improves the efficacy of BMP-4 for promoting adipogenesis. Additionally, sustained delivery of either FGF-1 or BMP-4 from alginate microgels resulted in lipid accumulation within larger vacuoles compared to induction media with or without growth factors (Fig. 5b–f). In summary, these results confirm that FGF-1 and BMP-4 released from alginate microgels are bioactive and pro-adipogenic.

Dual-stage growth factor release in 2D promotes adipogenesis

The effect of dual-stage growth factor release to induce adipogenic differentiation was assessed by delivery of FGF-1 and BMP-4 to hADSCs on TCPS over 7 days (Fig. 6). Total lipid accumulation, cell growth rate, and lipid accumulation per cell were quantified to demonstrate differences in adipogenesis between experimental groups (Fig. 6a-d). In all experiments, media was replaced with fresh growth or induction media without growth factors at day 3. In addition, all cells were exposed to alginate microgels (i.e. empty microgels were added to growth media and induction media). Cell growth rates and lipid accumulation in hADSCs were unaffected by the presence of empty alginate microgels (Fig. S1). Therefore, the observed differences in growth and lipid accumulation can be attributed to the efficacy and timing of FGF-1 and BMP-4 delivery. Short-term delivery of FGF-1 was achieved by direct addition to the induction media on day 0 followed by replacement with induction media without growth factors at day 3. Sustained delivery of BMP-4 and FGF-1 was achieved by adding alginate microgels at day 0.

Lipid accumulation per cell was significantly enhanced for cells cultured in induction media with sustained delivery of BMP-4 compared to growth media (Fig. 6d). The cell growth as measured by total dsDNA was not significantly different for cells with sustained exposure to BMP-4 compared to induction or growth media (Fig. 6c). BMP-4 signalling is required to induce terminal differentiation during adipogenesis,[53] which is consistent with these results. In contrast, either sustained or short-term delivery of FGF-1 significantly increased the cell growth rate, but did not significantly enhance lipid accumulation per cell. FGF-1 is known to stimulate preadipocyte proliferation. These results are supportive of the proposed differential effects of FGF-1 and BMP-4, with FGF-1 promoting preadipocyte commitment and proliferation (an early stage of adipogenesis) and with BMP-4 promoting terminal differentiation (a late stage of adipogenesis).

We then explored two temporal profiles for delivery of FGF-1 and BMP-4 in combination. In one case, sustained release of FGF-1 from microgels and BMP-4 from microgels was used to expose cells to both factors for the duration of 7 days. In the second case, short-term delivery of FGF-1 (days 0 to 3) was combined with sustained delivery of BMP-4 from microgels. This dual-stage experimental design exposes cells to higher concentrations of FGF-1 at early times and higher concentrations of BMP-4 at later times. While sustained co-delivery of FGF-1 and BMP-4 did not increase lipid accumulation per cell, the dual-stage delivery of FGF-1 and

BMP-4 resulted in markedly increased lipid accumulation per cell (Fig. 6d). Interestingly, the cell growth rate was not affected by sustained co-delivery of growth factors; however, the growth rate was significantly decreased by dual-stage delivery of growth factors (Fig. 6c). Typically, cell proliferation is stalled prior to terminal differentiation,[54] and therefore cell growth rates are expected to decrease when cells undergo terminal adipogenesis.

Sustained delivery of FGF-1, BMP-4, or the combination promoted lipid accumulation into larger lipid vacuoles, indicating differentiation of these cells toward a white-like adipocyte phenotype (Fig. 6a).[55] In contrast, dual-stage release of FGF-1 and BMP-4 promoted greater lipid accumulation in numerous, small lipid vacuoles, indicating differentiation of these cells toward a brown-like adipocyte phenotype (Fig. 6a).[55] Taken together, these results suggest that sustained BMP-4 delivery promotes terminal adipocyte differentiation, but that sustained FGF-1 delivery down regulates the process by promoting cell growth and stalling the terminal differentiation phase. Thus, short-term FGF-1 delivery may be required to enable terminal differentiation during adipogenesis. These results encourage further exploration and optimization of the total and relative growth factor concentrations and exact timing of delivery for induction of adipogenesis. In summary, these data confirm our hypothesis that dual-stage growth factor release can influence both the total amount and type of lipid accumulation during adipogenesis.

Dual-stage growth factor release in 3D promotes adipogenesis

We next explored the delivery of FGF-1 and BMP-4 in a 3D culture system. Dual-stage growth factor release was achieved by co-encapsulating three components into the MITCH material: (1) hADSCs, (2) FGF-1, and (3) alginate microgels loaded with BMP-4 (Fig. 7). To minimize the potential confounding effect of the material mechanical properties on induction of adipogenesis, the total volume fraction of alginate microgels was kept constant across all experiments, where empty alginate microgels were embedded within MITCH in the no growth factor control cases. Similar to the 2D experimental design, media was replaced with fresh growth or induction media without growth factors at day 3. Therefore, observed differences in lipid accumulation between experimental groups can be attributed to the presence and timing of delivery of FGF-1 and/or BMP-4.

Total lipid accumulation significantly increased when hADSCs were cultured within 3D MITCH compared to 2D TCPS cultures, regardless of growth factor delivery (Fig. 6b, 7b, Fig. S2). Conversely, cell growth rates significantly decreased for all 3D cultures, regardless of growth factor delivery (Fig. 6c, 7c, Fig. S2). Thus, when matched to identical growth factor delivery conditions, the 3D cultures resulted in a more than 10-fold increase in lipid accumulation per cell compared to their 2D culture counterparts (Fig. 6d, 7d, Fig. S2). In the absence of alginate microgels, cell proliferation was still decreased for 3D MITCH cultures relative to 2D TCPS cultures (Fig. S3). Taken together, these data confirm that culture dimensionality can greatly impact cell proliferation and differentiation.

We then examined adipogenesis for various growth factor delivery profiles within 3D MITCH cultures. Dual-stage delivery of FGF-1 and BMP-4 within 3D MITCH cultures significantly increased lipid accumulation per cell compared to all other experimental growth factor delivery groups (Fig. 7d). As in the 2D TCPS cultures, this enhanced lipid accumulation was accompanied by a significant decrease in cell growth rate (Fig. 7c).

Qualitative observations of the lipid accumulation in 3D MITCH provide further insight into potential variation in the type of adipocyte differentiation (i.e. white vs. brown). Lipid accumulation in hADSCs cultured within MITCH occurs by formation of numerous, small lipid vacuoles, indicating differentiation toward brown adipocytes (Fig. 7a). These results demonstrate that the combined effects of 3D MITCH culture with dual-stage delivery of FGF-1 and BMP-4 significantly enhance lipid accumulation in hADSCs, demonstrating more robust induction of adipogenesis.

Analysis of preadipocyte and adipocyte markers by qPCR

To further quantify differences in adipocyte differentiation, we measured the expression of mature mRNA transcripts for adipogenesis transcriptional regulators (C/EBPβ, C/EBPα, and PPARɣ) and adipocyte-associated proteins (FABP4, GLUT4, Leptin, and UCP1) relative to the housekeeping gene, GAPDH (Fig. 8). Similar to the observed increase in total lipid accumulation, relative mRNA of the aforementioned protein targets is significantly upregulated in hADSCs within 3D MITCH cultures compared to 2D TCPS cultures (Fig. 8, Fig. S4).

Significant differences were observed between experimental groups for multiple protein markers, with no single identifiable trend at day 7. C/EBPβ activation, followed by C/EBPα and PPARɣ activation, occurs during adipogenesis.[56] Therefore a sampling of these markers at a single time point cannot be indicative of maximal activation. In 3D MITCH cultures, all three transcriptional regulators were significantly upregulated for hADSCs exposed to induction media compared to growth media, demonstrating the adipogenic potential of these cultures (Fig. 8a). Dual-stage delivery of FGF-1 and BMP-4 significantly increased C/EBPβ, but not C/EBPα or PPARɣ, compared to all other experimental groups (Fig. 8a). Mature, fully differentiated adipocytes show upregulation of C/EBPβ and repression of C/EBPα and PPARɣ, following insulin stimulation.[57] Notably, C/EBPα activation is not required for brown adipocyte differentiation.[58] Therefore, the resulting mRNA profile seen here from dual-stage delivery of FGF-1 and BMP-4 suggests that these cells are more similar to mature, insulin-sensitive, brown-like adipocytes than the cells in the other experimental conditions.

We further analyzed expression of downstream targets of the adipogenic transcriptional regulators, FABP4 and GLUT4.[12,71] In 3D MITCH cultures, both FABP4 and GLUT4 mRNA were significantly increased for cells exposed to induction media alone, sustained co-delivery of FGF-1 and BMP-4, and dual-stage delivery of FGF-1 and BMP-4, compared to growth media (Fig. 8b). Interestingly, FABP4 mRNA increased at least 2-fold in hADSCs cultured in 3D MITCH compared to 2D TPCS cultures, regardless of growth factor delivery (Fig. S4). These results support the observed increase in lipid accumulation, as FABP4 binds and transports long chain fatty acids in preadipocytes, as well as white and brown adipoctyes.[59] GLUT4 activity is essential for whole body glucose homeostasis in response to insulin stimulation and is acquired during the late stages of terminal differentiation during

adipogenesis.[60] Upregulation of GLUT4 suggests that these cell populations contain terminally differentiated adipocytes with insulin sensitivity.

Lastly, we analyzed expression of Leptin and UCP1 to determine potential differences in the types of adipocytes present (Fig. 8c). UCP1 is a functional marker of brown adipocytes and is upregulated following insulin stimulation; UCP1 is typically not detectable in white adipoctyes.[61] Leptin is expressed during terminal differentiation of white adipocytes.[66] Therefore, relative differences between Leptin and UCP1 mRNA can be used to distinguish between brown, brown/white, and white adipocytes. In 3D MITCH cultures, dual-stage delivery significantly increased UCP1, but not Leptin, mRNA compared to growth media (Fig. 8c). Furthermore, dual-stage delivery of FGF-1 and BMP-4 significantly increased the relative expression of UCP1 over Leptin compared to all other experimental groups, suggesting hADSC differentiation toward brown adipocytes (Fig. S5). In contrast, simultaneous co-delivery of FGF-1 and BMP-4 significantly increased both Leptin and UCP1 mRNA compared to growth media (Fig. 8c, Fig. S5), suggesting hADSC differentiation toward brown/white adipocytes.[61] These results demonstrate that dual-stage delivery of FGF-1 and BMP-4 within 3D MITCH cultures alters the differentiation potential of hADSCs toward brown-like adipocytes.

Conclusions

To our knowledge, this is the first reported use of dual-stage delivery of FGF-1 and BMP-4 for induction of adipogenesis. The combination of 3D hADSC culture within MITCH hydrogels and dual-stage delivery of FGF-1 and BMP-4 enhances lipid accumulation and drives differentiation toward brown-like adipocytes. These biomimetic microenvironments with dual-stage growth factor release may be useful for *in vitro* models of disease progression and drug discovery as well as *in vivo* tissue engineering applications. In particular, the biomimetic model developed here may provide insight into the environmental cues that promote adipogenesis toward white, brown/white, or brown adipocytes. The ability to promote specific differentiation toward brown adipocytes is important for brown adipose tissue development and regulation of glucose homeostasis. An advantage of this 3D, dual-stage delivery platform is that the alginate microgels can be engineered independently from MITCH prior to encapsulation of bioactive factors. Therefore, this system could be used to deliver a broad range of bioactive factors with distinct release profiles within a tunable 3D hydrogel to mimic a variety of native microenvironments.

Acknowledgements

Notes

[a] Department of Bioengineering, Stanford University, Stanford, California 94305, United States
[b] Department of Materials Science and Engineering, Stanford University, Stanford, California 94305, United States

References

1 D. E. Discher, D. J. Mooney, and P. W. Zandstra, *Science*, 2009, **324**, 1673.

2 M. F. Brizzi, G. Tarone, and P. Defilippi, *Curr Opin Cell Biol.*, 2012, **24**, 645.

3 A. K. Dutta and R. C. Dutta, *Biotechnol Adv.*, 2009, **J27**, 334.

4 D. A. Wang and Y. Peck, *Expert Opin Drug Deliv.*, 2013, **10**, 369.

5 M. W. Tibbitt and K. S. Anseth, *Sci Transl Med.*, 2012, **14**, 24.

6 P. Zorlutuna, N. E. Vrana, A. Khademhosseini, *IEEE Rev Biomed Eng.* 2013, **6**, 47.

7 J. A. Burdick and G. Vunjak-Novakovic, *Tissue Engineering Part A.*, 2009, **15**, 205.

8 M. P. Lutolf, P. M. Gilbert, and H. M. Blau, *Nature*, 2009, **462**, 433.

9 L. G. Griffith, and G. Naughton, *Science*, 2002, **295**, 1009.

10 D. Seliktar, *Science*, 2012, **336**, 1124.

11 D. Sengupta and S. C. Heilshorn, *Tissue Eng Part B Rev.*, 2010, **16**, 285.

12 A. G. Cristanchol and M. A. Lazar, *Nat Rev Mol Cell Biol.*, 2011, **12**, 722.

13 P.A. Zuk, M. Zhu, P. Ashjian, D. A. De Ugarte, J. I. Huang *et al.*, *Mol Biol Cell.*, 2002; **13**, 4279.

14 G. Yu, Z. E. Floyd, X. Wu, T. Hebert, Y. D. Halvorsen *et al.*, *Methods Mol Biol.*, 2011, **702**, 193.

15 E. D. Rosen and O. A. MacDougald, *Nat Rev Mol Cell Biol.*, 2006, **7**, 885.

16 D.H. Stacey, S.E. Hanson, G. Lahvis, K.A. Gutowski, and K.S. Masters, *Tissue Eng Part A.*, 2009; **15**, 3389.

17 K.C. O'Connor, H. Song, N. Rosenzweig, and D.A. Jansen, *Biotechnol Lett.*, 2003, **25**, 1967.

18 J. H. Choi, J. M. Gimble, K. Lee, K. G. Marra, J. P. Rubin *et al.*, *Tissue Eng Part B Rev.*, 2010, **16**, 413.

19 J. J. Marler, A. Guha, J. Rowley, R. Koka, D. J. Mooney *et al.*, *Plast Reconstr Surg.*, 2000, **105**, 2049.

20 S. W. Kang, B. H. Cha, H. Park, K. S. Park, K. Y. Lee, *et al.*, *Macromol Biosci.*, 2011, **11**, 673.

21 N. Huebsch, P. R. Arany, A. S. Mao, D. Shvartsman, O. A. Ali, *et al.*, *Nature Mater.*, 2010, **9**, 518.

22 F. P. Brandl, A. K. Seitz, J. K. Tessmar, T. Blunk, and A. M. Göpferich, *Biomaterials*, 2010, **31**, 3957.

23 C. T. Wong Po Foo, J. S. Lee, W. Mulyasasmita, A. Parisi-Amon, and S.C. Heilshorn, *Proc Natl Acad Sci U S A.*, 2009, **106**, 22067.

24 W. Mulyasasmita, J. S. Lee, and S.C. Heilshorn, *Biomacromolecules*, 2011, **12**, 3406.

25 A. Parisi-Amon, W. Mulyasasmita, C. Chung, and S.C. Heilshorn, *Adv Healthc Mater.*, 2013, **2**, 428.

26 N. K. Varde and D. W. Pack. *Expert Opin Biol Ther.*, 2004, **4**, 35.

27 V. R. Sinha and A. Trehan. *J Control Release*, 2003, **90**, 261.

28 X. M. Lam, E. T. Duenas, A. L. Daugherty, N. Levin, and J. L. Cleland, *J Control Release*, 2000, **67**, 281.

29 X. Wang, E. Wenk, X Zhang, L. Meinel, G. Vunjak-Novakovic *et al.*, *J Control Release*, 2009, **134**, 81.

30 P. C. Bessa, R. Machado, S. Nürnberger, D. Dopler, A. Banerjee, *et al.*, *J Control Release*, 2010, **142**, 312.

31 G. T. Franzesi, B. Ni, Y. Ling, and A. Khademhosseini, *J Am Chem Soc.*, 2006, **128**, 15064.

32 S. Xu, Z. Nie, M. Seo, P. Lewis, E. Kumacheva *et al.*, *Angew Chem Int Ed Engl.*, 2005, **44**, 724.

33 F. Ungaro, M. Biondi, I. d'Angelo, L. Indolfi, F. Quaglia, *et al.*, *J Control Release*, 2006, **113**, 128.

34 M. H. Sheridan, L. D. Shea, M. C. Peters, and D. J. Mooney, *J Control Release*, 2000, **64**, 91.

35 S. M. Jay and W. M. Saltzman, *J Control Release*, 2009, **134**, 26.

36 T. P. Richardson, M. C. Peters, A. B. Ennett, and D. J. Mooney, *Nature Biotechnol.*, 2001, **19**, 1029.

37 I. Freeman and S. Cohen, *Biomaterials*, 2009, **30**, 2122.

38 L. Hutley, W. Shurety, F. Newell, R. McGeary, N. Pelton, *et al.*, *Diabetes*, 2004, **53**, 3097.

39 J. W. Jonker, J. M. Suh, A. R. Atkins, M. Ahmadian, P. Li *et al.*, *Nature*, 2012, **485**, 391.

40 M. Suenaga, N. Kurosawa, H. Asano, Y. Kanamori, T. Umemoto *et al.*, *Cytokine*, 2013, **64**, 138.

41 Q. Q. Tang, T. C. Otto, and M. D. Lane. *Proc Natl Acad Sci U S A.*, 2004, **101**, 9607.

42 X. Luo, L. J. Hutley, J. A. Webster, Y. H. Kim, D. F. Liu *et al.*, *Diabetes*, 2012, **61**, 124.

43 T. Ward, M. Faivre, M. Abkarian and H. Stone, *Electrophoresis*, 2005, **26**, 3716.

44 E. Doherty, C. Kan, and A. Barron, *Electrophoresis*, 2003, **24**, 4170.

45 R. Seemann, M. Brinkmann, T. Pfohl, and S. Herminghaus, Reports on Progress in Physics, 2012, **75**, 016601.

46 S. Preibisch, S. Saalfeld, and P. Tomancak, *Bioinformatics*, 2009, **25**, 1463.

47 K. J. Livak and T.D. Schmittgen, *Methods*, 2001, **25**, 402.

48 Y.A. Morch, I. Donati, B. L. Strand, and G. Skjak-Braek, *Biomacromol.*, 2006, **7**, 1471.

49 J. Rejman, V. Oberle, I. S. Zuhorn, and D. Hoekstra, *Biochem J.*, 2004, **377**, 159.

50 S. Y. Fu, X. Q. Feng, B. Lauke, and Y. W. Mai, *Composites Part B: Eng.*, 2008, **39**, 933.

51 J. P. Winer, P. A. Janmey, M. E. McCormick, and M. Funaki, *Tissue Eng Part A.*, 2009, **15**, 147.

52 C. H. Widberg, F. S. Newell, A. W. Bachmann, S. N. Ramnoruth, M. C. Spelta, *et al. Am J Physiol Endocrinol Metab.*, 2009, **296**, E121.

53 H. Huang, T. J. Song, X. Li, Q. He, M. Liu *et al.*, *Proc Natl Acad Sci U S A.*, 2009, **106**, 12670.

54 L. Zhu and A. I. Skoultchi, *Curr Opin Genet Dev.*, 2001, **11**, 91.

55 S. Cinti. *Ann Med.*, 2001, **43**, 104.

56 T. M. Loftus and M. D. Lane, *Curr Opin Genet Dev.*, 1997, **7**, 603.

57 O. A. MacDougald and M. D. Lane, *Annu. Rev. Biochem.*, 1995, **64**, 345.

58 H. G. Linhart, K. Ishimura-Oka, F. DeMayo, T. Kibe, B. Poindexter *et al.*, *Proc Natl Acad Sci U S A.*, 2001, **98**, 12532.

59 T. Shan, W. Liu, and S. Kuang, *FASEB J.*, 2013, **27**, 277.

60 S. Huang and M. P. Czech, *Cell Metab.*, 2007, **5**, 237.

61 J. Wu, P. Cohen, and B. M. Spiegelman, *Genes Dev.*, 2013, **27**, 234.

Figure Captions

Figure 1. Formation of alginate microgels and encapsulation within a protein-engineered hydrogel for temporally controlled release of soluble factors. (a) Illustration of on-chip droplet formation of an aqueous phase containing alginate and soluble factors, off-chip crosslinking of alginate microgels to sequester the soluble factors, and encapsulation of alginate microgels within a mixing induced, two-component hydrogel (MITCH). MITCH forms through heteroassembly, during which two different polypeptide chains containing complementary molecular recognition domains form physical crosslinks by hydrogen bonding. (b) *In vitro* release profiles of FGF-1 released from MITCH embedded with empty microgels (*green circles*) and BMP-4 released from alginate microgels encapsulated within MITCH (*blue diamonds*).

Figure 2. Alginate microgel characterization of loading efficiency and size. (a) Encapsulation efficiency increased significantly with increasing Dextran molecular weight, * $p < 0.05$. (b) Alginate microgel size was not significantly affected by Dextran molecular weight or charge; the average diameter (d ± S.D.) and coefficient of variance (CV) are listed. (c) Representative phase contrast micrograph of alginate microgels containing 40 kD Dextran-FITC, crosslinked in 400 mM $BaCl_2$.

Figure 3. Rheology of MITCH embedded with alginate microgels. (a) Shear modulus of MITCH decreases with decreasing volume fraction of alginate microgels, * $p < 0.05$. (b) Viscosity of MITCH containing 25 v/v% microgels upon multiple cycles of shear-thinning and recovery. (c) Storage (G') and loss (G'') moduli before and after shear-thinning, demonstrating the self-healing properties of MITCH embedded with alginate microgels.

Figure 4. Release kinetics of soluble factors delivered from alginate microgels. *In vitro* release profiles for soluble factors were determined for Dextran-FITC molecules with variable molecular weights, FGF-1, and BMP-4, released from 8 wt% alginate microgels crosslinked in a 400 mM $BaCl_2$ divalent ion bath. At long time points (a) the release rate is diffusion-based and dependent on molecular weight. At early time points (b) the release profile is linear for Dextran-FITC molecules and for both FGF-1 and BMP-4, with less than 30% of the encapsulated growth factor released by day 7. (c) High encapsulation efficiency of FGF-1 and BMP-4 is demonstrated when loading 2 μg/ml of growth factors into alginate microgels. The final concentrations of FGF-1 and BMP-4 used for release studies is approximately 1.7 μg/ml.
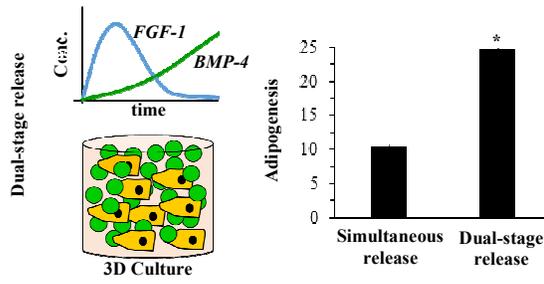
Figure 5. Bioactivity of soluble factors delivered from alginate microgels. (a) Lipid accumulation per cell was determined at day 7 by normalizing total Oil Red O absorbance to total dsDNA. The lipid accumulation per cell resulting from sustained delivery of FGF-1 and BMP-4 from microgels was normalized to the lipid accumulation per cell resulting from dose delivery of FGF-1 and BMP-4 directly to the induction media, * $p < 0.01$. Representative phase contrast images of Oil Red O staining of accumulated lipids in hADSCs at day 7 for (b) sustained delivery of FGF-1 from microgels (c) sustained delivery of BMP-4 from microgels (d) adipogenic induction media (IM) alone (e) dose delivery of FGF-1 and (f) dose delivery of BMP-4.
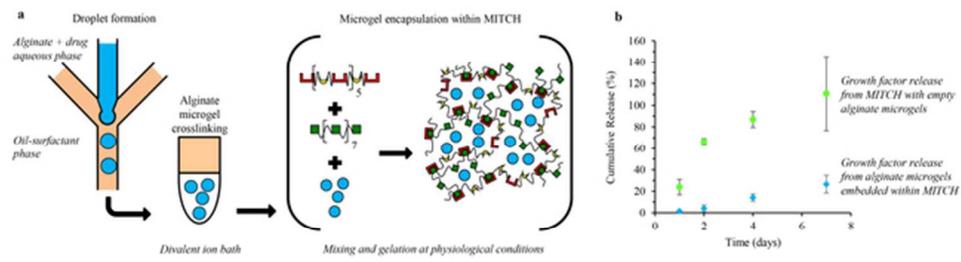
Figure 6. 2D *in vitro* adipogenesis of hADSCs by dual-stage delivery of FGF-1 and BMP-4. (a) Representative images of 7 day TCPS cultures; lipid accumulation shown by Oil Red O staining and phase contrast microscopy (left panels) and cell nuclei shown by DAPI staining and fluorescence microscopy (right panels). (b) Lipid accumulation was estimated by Oil Red O quantification. (c) The total number of cells was estimated by quantifying total dsDNA. (d) The estimated lipid accumulation per cell was determined by normalizing Oil Red O absorbance to total dsDNA. Statistical analysis results are denoted by lower case letters, different individual letters denote significant differences between experimental groups within each assay, $p < 0.05$.

Figure 7. 3D *in vitro* adipogenesis of hADSCs by dual-stage delivery of FGF-1 and BMP-4. (a) Representative images of 7 day cultures in MITCH with embedded alginate microgels; lipid accumulation shown by Oil Red O staining and phase contrast microscopy (left panels) and cell nuclei shown by DAPI staining and fluorescence microscopy (right panels). (b) Lipid accumulation was estimated by Oil Red O quantification. (c) The total number of cells was estimated by quantifying total dsDNA. (d) The estimated lipid accumulation per cell was determined by normalizing Oil Red O absorbance to total dsDNA. Statistical analysis results are denoted by lower case letters, where different individual letters denote significant differences between experimental groups within each assay, $p < 0.05$.
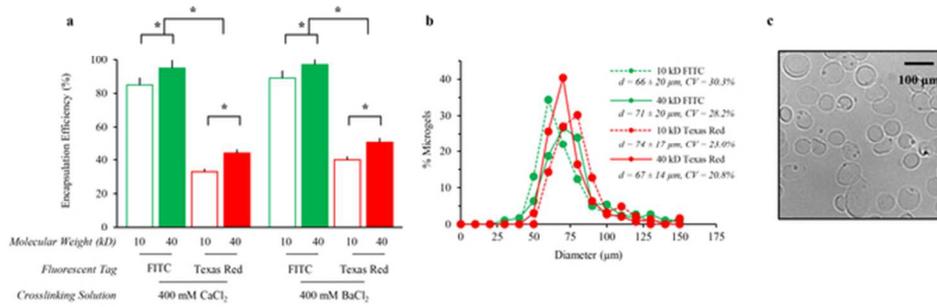
Figure 8. Relative concentration of mature mRNA transcripts for adipogenesis transcriptional regulators and mature adipocyte associated proteins. qPCR of cell lysates at day 7 was used to determine relative mRNA concentrations between negative control, positive control, and experimental groups in 2D TCPS and 3D MITCH cell cultures. A one-way analysis of variance with Tukey Post-hoc analysis revealed significant differences between experimental groups within TCPS and MITCH cultures. (a) Relative mRNA concentrations of adipogenic transcriptional regulators C/EBPα, C/EBPβ, and PPARγ. (b) Relative mRNA concentrations of general adipocyte markers FABP4 and GLUT4. (c) Relative mRNA concentrations of brown adipocyte makers, Leptin and UCP1, respectively. Statistical analysis results are denoted by lower case letters, where different individual letters denote significant differences between experimental groups. Within TCPS or MITCH cultures, statistical significance was independently assessed for each gene, $p < 0.05$.

Biomimetic microenvironments from hydrogels can be used to promote *in vitro* stem cell differentiation. We developed a strategy for dual-stage delivery of fibroblast growth factor 1 (FGF-1) and bone morphogenetic protein 4 (BMP-4) within 3D cell cultures to promote adipogenesis in human adipose-derived stromal cells.
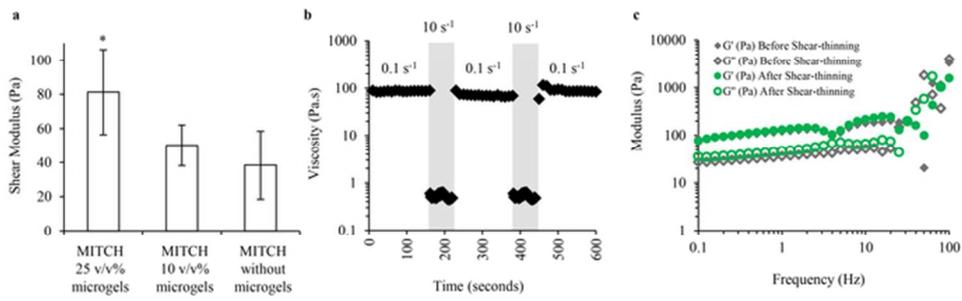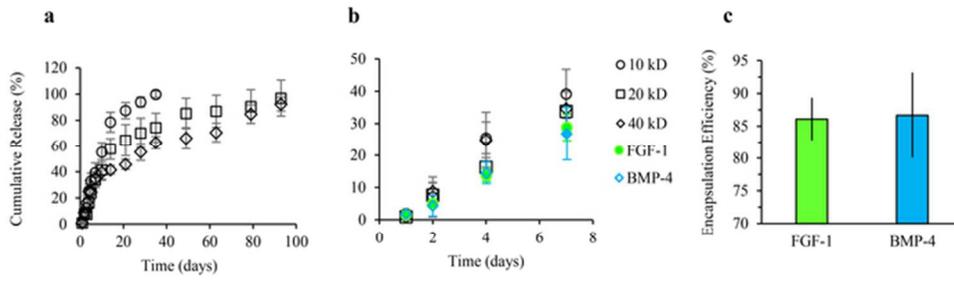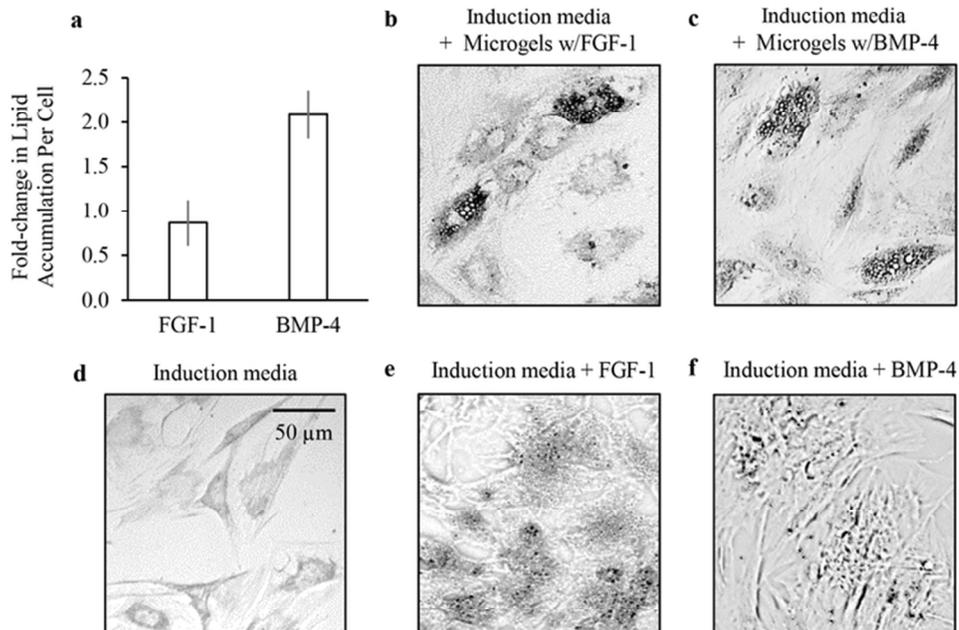
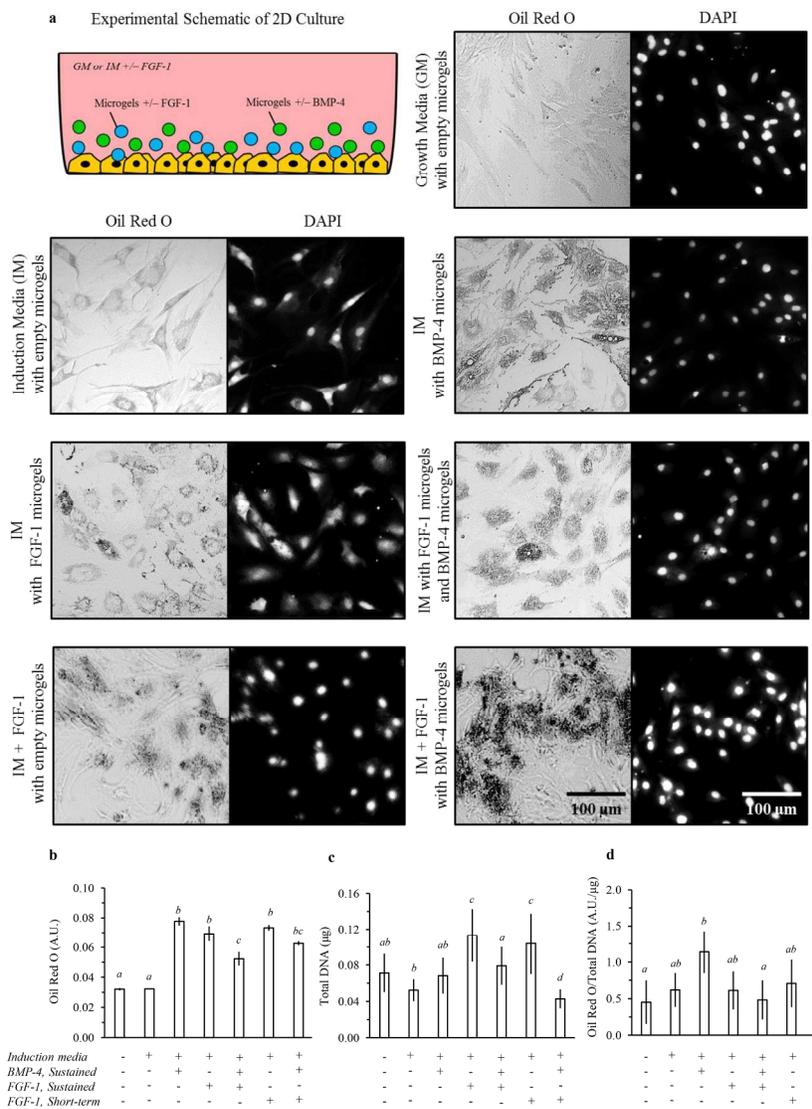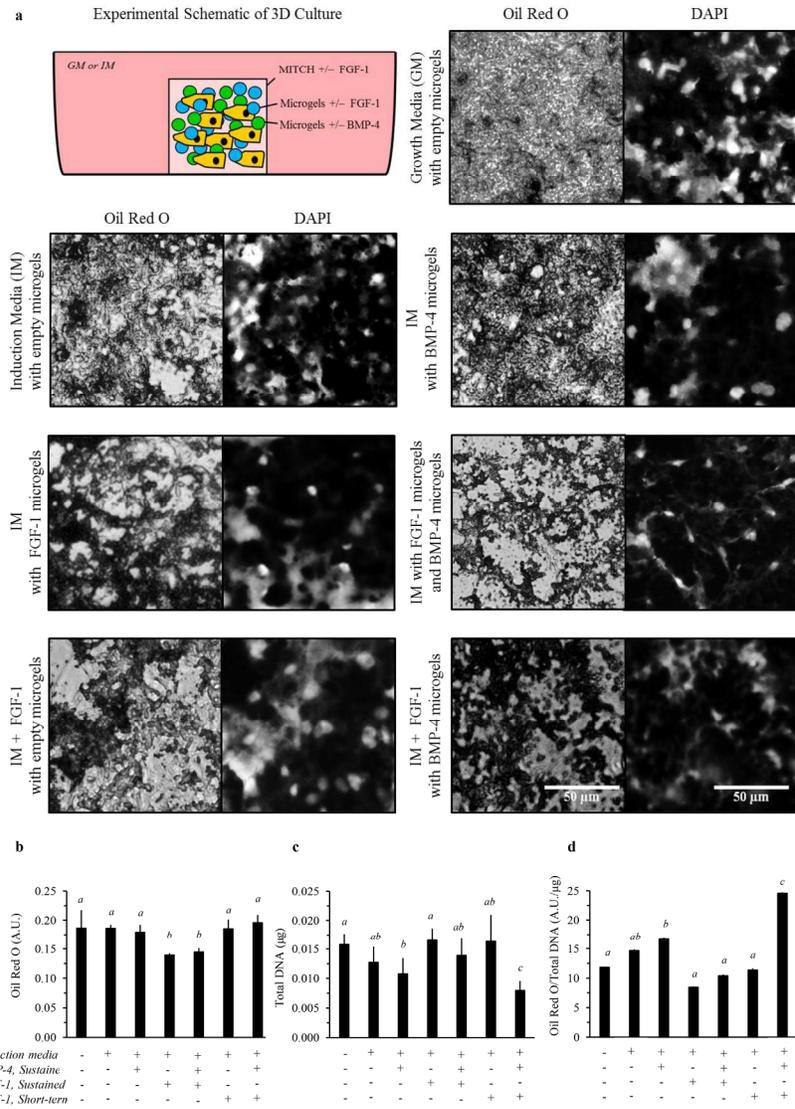56x18mm (300 x 300 DPI)

60x21mm (300 x 300 DPI)
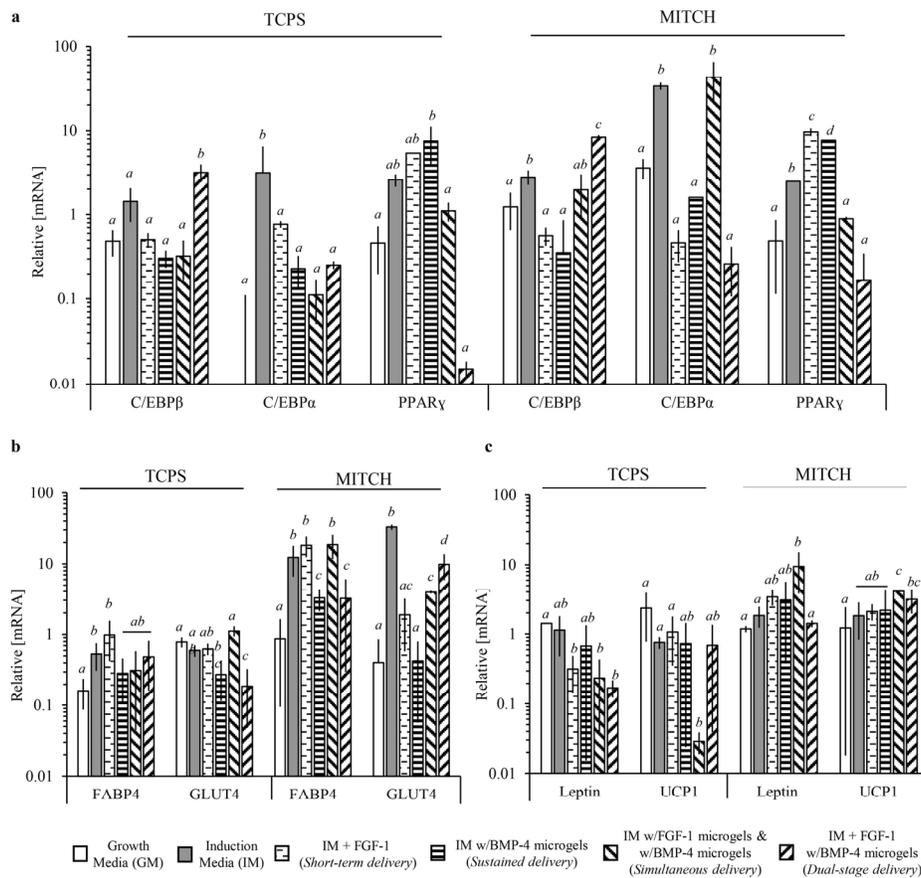
60x21mm (300 x 300 DPI)

60x21mm (300 x 300 DPI)

a

b   Induction media
    + Microgels w/FGF-1

c   Induction media
    + Microgels w/BMP-4

d   Induction media

e   Induction media + FGF-1

f   Induction media + BMP-4

66x53mm (300 x 300 DPI)

a Experimental Schematic of 2D Culture

Oil Red O   DAPI

GM or IM +/− FGF-1

Microgels +/− FGF-1   Microgels +/− BMP-4

Growth Media (GM) with empty microgels

Oil Red O   DAPI

Induction Media (IM) with empty microgels

IM with BMP-4 microgels

IM with FGF-1 microgels

IM with FGF-1 microgels and BMP-4 microgels

IM + FGF-1 with empty microgels

IM + FGF-1 with BMP-4 microgels

100 μm   100 μm

b

Oil Red O (A.U.)

Induction media	-	+	+	+	+	+	+
BMP-4, Sustained	-	-	+	-	+	-	+
FGF-1, Sustained	-	-	-	+	+	-	-
FGF-1, Short-term	-	-	-	-	-	+	+

c

Total DNA (μg)

d

Oil Red O/Total DNA (A.U./μg)

216x274mm (300 x 300 DPI)

216x274mm (300 x 300 DPI)

158x147mm (300 x 300 DPI)